

Original paper

Detailed insight into magnetic resonance assessment of Ménière's disease – description of methodology and imaging findings in a case series

Emilia Wnuk^{1,A,B,D,E,F}, Magdalena Lachowska^{2,A,D,E,F}, Agnieszka Jasińska-Nowacka^{2,B,D,E}, Edyta Maj^{1,D,E},
Olgierd Rowiński^{1,D,E}, Kazimierz Niemczyk^{2,A,E}

¹2nd Department of Clinical Radiology, Medical University of Warsaw, Poland

²Department of Otorhinolaryngology, Head and Neck Surgery, Medical University of Warsaw, Poland

Abstract

Purpose: The study aimed to describe the methodology and detailed interpretation of magnetic resonance imaging (MRI) in patients with Ménière's disease (MD).

Material and methods: MRIs were performed on a 3T scanner. The three-dimensional fluid-attenuated inversion recovery (3D-FLAIR) sequence 4 hours after a double dose of intravenous contrast was added to the standard MRI protocol in patients with clinically diagnosed MD. MRI findings of 7 patients with unilateral MD were analysed using 2 qualitative grading systems by Barath and Bernaerts.

Results: In MRI, the following changes in the group of patients with MD were observed: lack of endolymphatic hydrops (cases #1 and #7), various grades of cochlear hydrops (cases #2 and #3), various grades of vestibular hydrops (cases #4, #5, and #6), endolymphatic hydrops herniation into the semi-circular canal (case #6), and more robust perilymphatic enhancement (case #7).

Conclusions: In patients with MD, endolymphatic hydrops can be studied on MRI using 3D-FLAIR delayed post-contrast images. The qualitative grading system may be easily used in endolymphatic hydrops assessment. Recently described new radiological signs of MD such as increased perilymphatic enhancement of the cochlea and an extra low-grade VH may increase MD diagnosis sensitivity. MRI not only supports the clinical diagnosis of MD but also may help to understand its pathophysiology.

Key words: Ménière's disease, endolymphatic hydrops, inner ear, magnetic resonance imaging, 3D-FLAIR.

Introduction

Ménière's disease (MD) is a chronic inner ear disorder characterized by spontaneous vertigo episodes, fluctuating low-frequency hearing loss, tinnitus, and fullness in the ear [1]. In 1861 Prosper Ménière was the first to report that the inner ear disease might be a source of symptoms typical for this disease [2]. About 80 years later, Hallpike and Cairns [3] in England and Yamakawa [4] in Japan independently described the dilatation of endolymphatic structures in post-mortem temporal bone sections of patients with MD. For many years, the possibility of *in vivo* assess-

ment of the endolymphatic hydrops (EH) did not exist. The diagnosis of MD was based on the patient's symptoms, clinical findings, and functional tests. Guidelines for MD diagnosis were formulated in 1995 by the American Academy of Otolaryngology-Head and Neck Surgery [5]. According to these criteria, a definite MD could be recognized only post-mortem. In 2015 this scale was simplified by the Barany society [1,6]; definite MD is recognized when the combination of symptoms and audiometrically proved sensorineural hearing loss is present and no other underlying vestibular pathology exists (Table 1); thus, it is a diagnosis of exclusion.

Correspondence address:

Prof. Magdalena Lachowska, MD, PhD, Department of Otorhinolaryngology, Head and Neck Surgery, Medical University of Warsaw, 1a Banacha St., 02-097 Warsaw, Poland, phone: +48 22 599 25 21, e-mail: mlachowska@wum.edu.pl

Authors' contribution:

A Study design · B Data collection · C Statistical analysis · D Data interpretation · E Manuscript preparation · F Literature search · G Funds collection

Table 1. American Academy of Otolaryngology-Head and Neck Surgery (AAO-HNS) criteria for the diagnosis of Ménière's disease (MD) described in 2015 [1,5]

Definite MD	<ul style="list-style-type: none"> • Two or more spontaneous episodes of vertigo, each lasting 20 min to 12 h • Audiometrically documented low- to mid-frequency sensorineural hearing loss in one ear, defining the affected ear on at least one occasion before, during, or after one of the episodes of vertigo • Fluctuating aural symptoms (hearing, tinnitus, or fullness) in the affected ear • Not better accounted for by another vestibular diagnosis
Probable MD	<ul style="list-style-type: none"> • Two or more episodes of vertigo or dizziness, each lasting 20 min to 24 h • Fluctuating aural symptoms (hearing, tinnitus, or fullness) in the affected ear • Not better accounted for by another vestibular diagnosis

Consequently, radiology's role was to rule out other pathologies that might cause symptoms similar to those of MD. With the development of the magnetic resonance imaging (MRI) technique, especially very high-field scanners (3 Tesla), the visualization of endolymphatic structures has become possible. Nakashima and Naganawa [7] intratympanically administered contrast, which moved into the perilymphatic space of the inner ear so that non-contrasted endolymphatic structures were clearly visible on three-dimensional fluid-attenuated inversion recovery T2 (3D-FLAIR) sequence. A few years later, they improved this method using a double dose of intravenously administered contrast [8]. Once this method became more accessible, a great perspective of inner ear research opened up. Several scales of EH assessment were proposed: first, semi-quantitative described by Nakashima *et al.* [9], next volumetric by Gürkov *et al.* [10], a qualitative system by Barath *et al.* [11], followed by a saccular morphology-based method by Attye *et al.* [12], and a four-grade staging system recently published by Bernaerts *et al.* [13].

Our study aimed to describe the methodology and detailed interpretation of MRI findings in patients with MD.

Material and methods

The local Ethics Committee reviewed and approved the study protocol at the institution where the study was conducted (KB/110/2019). The project conforms to the Code of Ethics of the World Medical Association (Declaration of Helsinki). All patients gave their written informed consent for participation in the study.

In this study, the presented patients were included as examples to illustrate the methodology and detailed interpretation of MRI results. All the included patients were

diagnosed with MD according to AAO-HNS criteria [1]. Seven patients (4 females and 3 males) with definite unilateral MD at different EH stages were enrolled in this study. The mean age at the time of the examination was 50.7 years (34-68 range).

All patients underwent an MRI study using a 3 Tesla MR scanner (Signa Architect, GE Healthcare, Milwaukee, USA) with a 16-channel phased array flex coil (GEM Flex Large coil, Neocoil, Pewaukee, USA). The examination was carried out in a supine position. Care was taken to tighten the coil as much as possible, considering patients' comfort and achieving the best image quality. The imaging protocol for MD included the following sequences: T2, T2 fluid-attenuated inversion recovery (T2 FLAIR), three-dimensional – fast-inflow steady-state acquisition (3D-FIESTA), three-dimensional – T1 (3D-T1), and three-dimensional fluid-attenuated inversion recovery T2 (3D-FLAIR). Post-contrast images were obtained shortly after administering a double dose (0.2 ml/kg) of gadobutrol (Gadavist; Bayer Schering Pharma AG, Berlin, Germany; 1.0 mmol/ml) using 3D-T1 sequence, and delayed post-contrast images were acquired 4 hours after contrast injection using 3D-FLAIR T2 sequence. The last sequence of 3D-FLAIR T2 with a double dose of contrast media was crucial for EH visualization and assessment. The detailed scan parameters are described in Table 2.

The MRI scans were analysed by 2 head and neck radiologists (the first and fourth authors) and by an otolaryngologist (the third author) using commercial imaging software (AW Server 3.2, GE Healthcare, Milwaukee, USA). EH was categorized using 2 grading systems: Barath [11] and Bernaerts [13] (Table 3). The assessment of the cochlear hydrops (CH) was performed at the level of the mid-modiolar area and the vestibular hydrops (VH)

Table 2. Detailed magnetic resonance sequence parameters of imaging protocol for Ménière's disease

Sequence	Plane	TR (ms)	TE (ms)	NEX	Matrix (mm)
T2	Axial and coronal	5385	120	2.0	416 × 416
T2 FLAIR	Axial	12 000	143	1.0	260 × 200
3D-FIESTA	Axial	9.3	3.0	1.0	480 × 480
3D-T1	Sagittal	6.9	2.8	1.0	256 × 256
3D-T2 FLAIR	Axial	7602	170	2.0	232 × 232

FLAIR – fluid-attenuated inversion recovery, 3D – three-dimensional, FIESTA – fast-inflow steady-state acquisition.

Table 3. Magnetic resonance imaging grading qualitative scales proposed by Barath [11] and modified by Bernaerts [13] for evaluation of the cochlear and vestibular endolymphatic hydrops

Severity of hydrops	Barath scale	Bernaerts scale
Cochlear endolymphatic hydrops (grade)		
Normal	0 – Barely visible/Invisible cochlear duct in enhancing scala vestibuli	
Mild	1 – Partial obstruction of scala vestibuli by dilated cochlear duct	
Severe	2 – Total obliteration of scala vestibuli by enlarged cochlear duct	
Vestibular endolymphatic hydrops		
Normal	0 – The saccule and utricle are separated, and the saccule is smaller than the utricle.	
Extra-low		1 – The saccule is equal or larger than the utricle but is not confluent with the utricle
Mild	1 – A confluence of saccule and utricle, a circular rim of perilymphatic space is visible	2 – A confluence of saccule and utricle, a circular rim of perilymphatic space is visible
Severe	2 – Total obliteration of the vestibular perilymphatic space by dilated endolymphatic structures	3 – Total obliteration of the vestibular perilymphatic space by dilated endolymphatic structures

at the level of the inferior part of the vestibule (below the mid-modiolar level). Furthermore, the degree of cochlear perilymphatic enhancement (PE) was evaluated in comparison to the contralateral (unaffected) side.

Results

Patients’ demographics and clinical characteristics are presented in Table 4.

In the first example (patient #1), a 60-year-old female with right-sided MD, on post-contrast 3D-FLAIR, a non-enhancing endolymphatic cochlear duct was invisible within the enhancing perilymphatic scala vestibuli and scala tympani – no CH was observed. Moreover, the vestibular structures, saccule and utricle, were clearly separated from each other. These images were interpreted as normal, meaning grade 0 CH and grade 0 VH in the Barath scale (Figure 1). Moreover, the saccule was smaller than the utricle, which was also graded 0 VH on the Bernaerts scale (Figure 2).

In the second example (patient #2), a 34-year-old female with right-sided MD, MRI revealed a cochlear duct

partially pushed away, enhancing the vestibular duct. It was classified as grade 1 CH (Figure 3). The vestibular structures were widened and confluent, but the vestibule’s enhancing rim was still visible, corresponding with grade 1 of VH in the Barath scale and grade 2 in the Bernaerts scale. In addition, the more robust enhancement of the basal turn of the cochlea was present on the affected side (Figure 4).

In the third example (patient #3), a 53-year-old female with right-sided MD, MRI revealed a significant cochlear EH. The enlarged scala media completely obstructed the scala vestibuli corresponding to grade 2 CH in Barath classifications; in addition, the more pronounced enhancement of the cochlea was observed (Figure 5). Moreover, VH grade 1 in the Barath scale was present, which corresponds with grade 2 in the Bernaerts scale.

In the fourth example (patient #4), a 36-year-old male with right-sided MD, the only abnormality observed on MRI was an enlarged saccule. This structure was bigger than the utricle but not yet confluent with it. According to the Barath criteria, this finding is considered normal grade 0 VH, but in the grading system proposed by Bern-

Table 4. Patients’ demographics and clinical characteristics of the study population [1,5]

Case No.	Gender	Age (years)	MD duration (years)	Affected ear	Hearing level (dB)	Hearing fluctuation (Y – Yes/N – No)	Tinnitus – Arenberg’s scale (0-6)	Vertigo attacks (in the last 6 months)	AAO-HNS classification (definite/probable)
1	F	60	6	Right	20.00	Y	2	0	Definite
2	F	34	19	Right	32.50	Y	3	6.33	Definite
3	F	53	13	Right	70.00	N	4	7.17	Definite
4	M	36	14	Right	18.75	Y	5	0.33	Definite
5	F	59	3	Right	43.75	N	3	4	Definite
6	M	45	5	Right	72.50	N	5	4	Definite
7	M	68	5	Right	61.25	Y	0	1	Definite

AAO-HNS – American Academy of Otolaryngology-Head and Neck Surgery

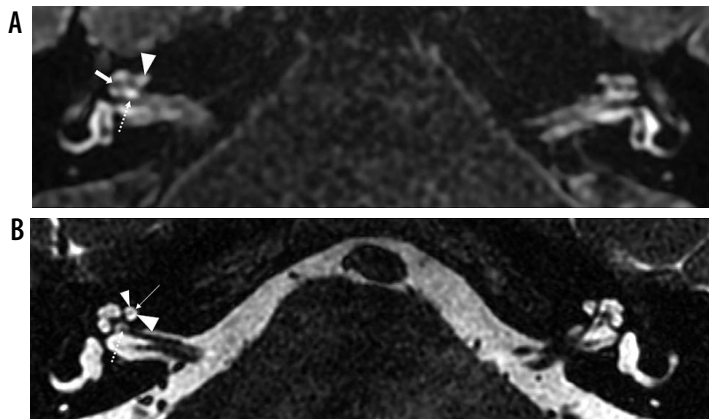


Figure 1. Magnetic resonance images of a 60-year-old female (patient #1) with right-sided clinically defined Ménière's disease. According to the Barath classification [11], the example case of the normal cochlea classified as grade 0 cochlear hydrops (CH). **A)** Delayed-postcontrast three-dimensional fluid-attenuated inversion recovery (3D-FLAIR) T2 axial image of both ears at the level of cochlear modiolus (marked with a dotted arrow). A non-enhancing cochlear duct is invisible in the enhanced scala vestibuli and scala tympani (marked with an arrowhead) – no signs of CH, the inter-scalar septum visible between the cochlear turns (marked with a thick arrow). **B)** Three-dimensional fast-inflow steady-state acquisition (3D-FIESTA) axial image of both ears demonstrates the normal anatomy of the inner ear structures at the cochlear modiolus level (marked with a dotted arrow). Osseous spiral lamina (marked with a thin arrow) separates scala vestibuli (marked with an arrowhead) from scala tympani (marked with a small arrowhead)

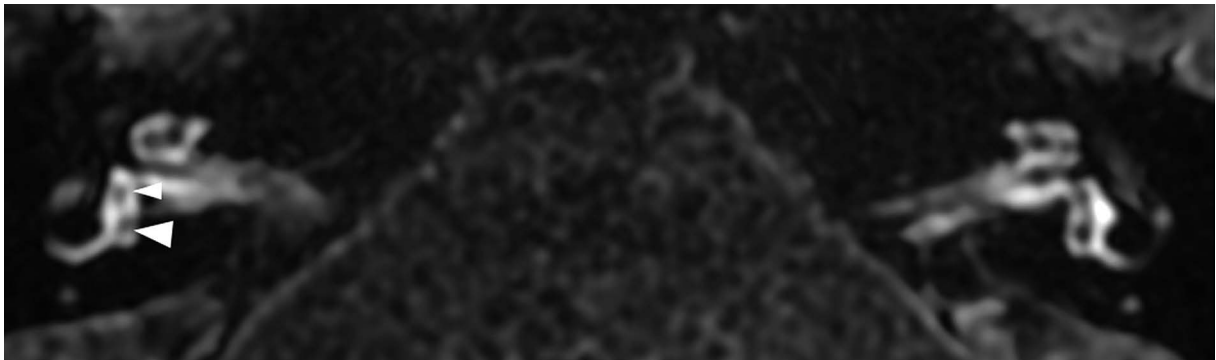


Figure 2. Magnetic resonance images of a 60-year-old female (patient #1) with right-sided clinically defined Ménière's disease. According to the Barath [11] and Bornaerts [13] classification, the example case of a normal vestibule classified as grade 0 vestibular hydrops. Delayed-postcontrast 3D-FLAIR T2 axial image of both ears below the level of modiolus (inferior part of the vestibule). The saccule (marked with a small arrowhead) and utricle (marked with an arrowhead) are well visualized. The saccule is smaller than the utricle, and endolymphatic structures encompass less than 50% of the vestibular area

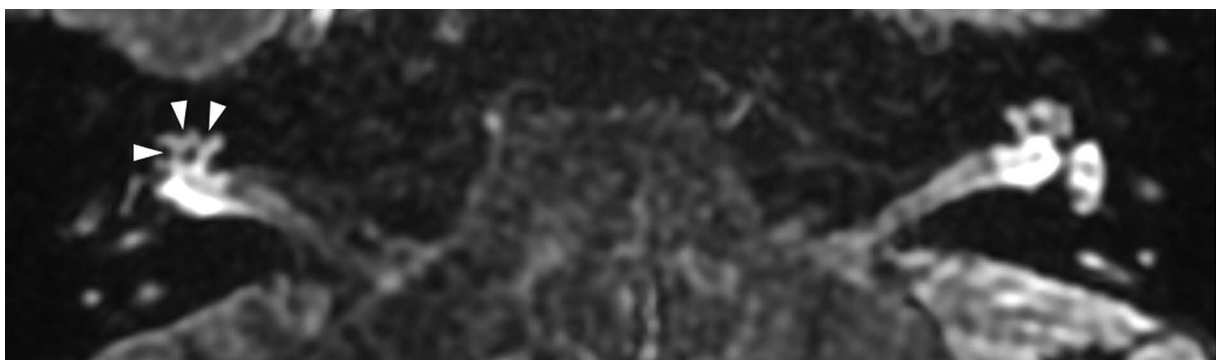


Figure 3. Magnetic resonance image of a 34-year-old female (patient #2) with right-sided clinically defined Ménière's disease. According to the Barath classification [11], it is an example case of grade 1 cochlear hydrops. Delayed-postcontrast 3D-FLAIR T2 axial image of both ears at the level of the cochlear modiolus. On the right side, a non-enhancing cochlear duct is visible as small dark nodules (marked with arrowheads) in the enhancing scala vestibuli; on the left side, normal left inner ear anatomy is presented for comparison

aerts, it was regarded as abnormal grade 1 VH (Figure 6). The CH or asymmetric PE was absent.

In the fifth example (patient #5), a 59-year-old female with right-sided MD, on MRI, vestibular endolymphatic

structures were enlarged and confluent, but circular perilymphatic space was still visible. It corresponded with grade 1 VH in the Barath scale and grade 2 in Bornaerts modification (Figure 7). Furthermore, in this patient,

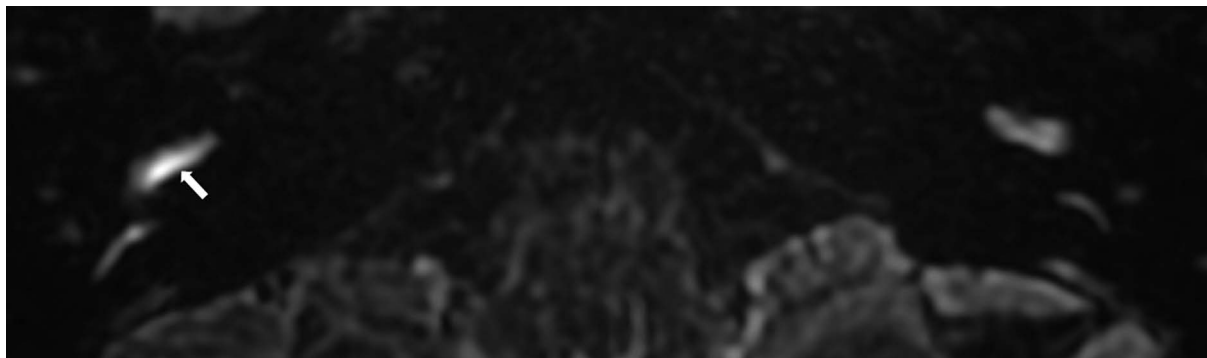


Figure 4. Magnetic resonance image of a 34-year-old female (patient #2) with right-sided clinically defined Ménière's disease. Delayed-postcontrast 3D-FLAIR T2 axial image of both ears at the level of the basal turn of the cochlea. The more robust enhancement of the basal cochlear turn on the affected right side (marked with an arrow) compared with normal perilymphatic enhancement on the left side

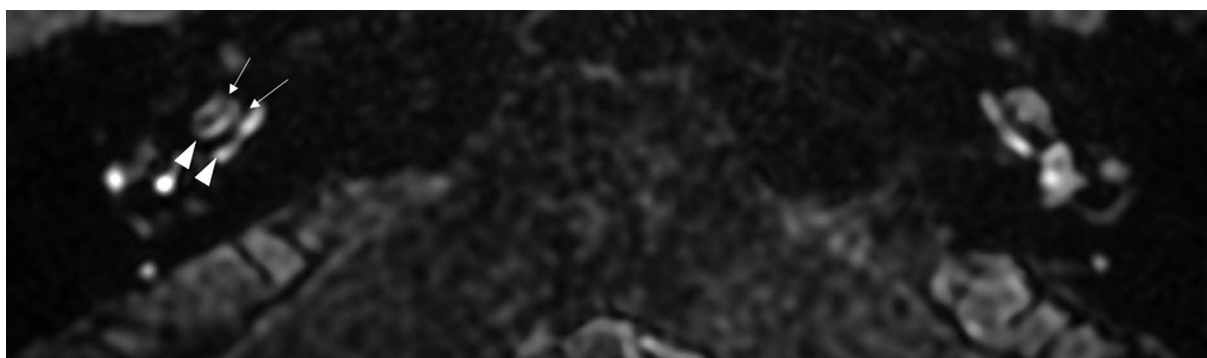


Figure 5. Magnetic resonance image of a 53-year-old female (patient #3) with right-sided clinically defined Ménière's disease. According to the Barath classification [11], it is an example case of grade 2 cochlear hydrops. Delayed-postcontrast 3D-FLAIR T2 axial image of both ears at the level of the cochlear modiolus. On the right side, a non-enhancing widened cochlear duct (marked with arrows) completely obstructs scala vestibuli, enhancing scala tympani (marked with arrowheads) resembling stripes

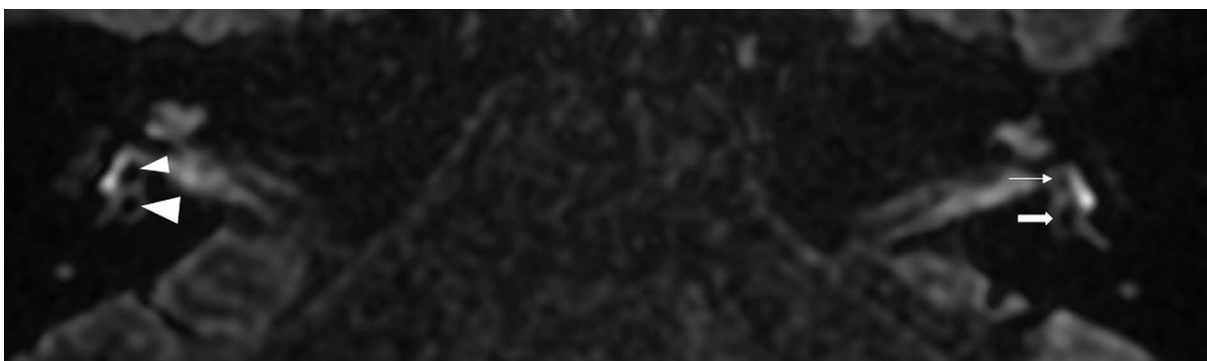


Figure 6. Magnetic resonance image of a 36-year-old male (patient #4) with right-sided clinically defined Ménière's disease. According to the Bernaerts classification [13], it is an example case of grade 1 (extra-low) vestibular hydrops. On the Barath scale [11], it is grade 0, presenting no signs of VH. Delayed-postcontrast 3D-FLAIR T2 axial image of both ears below the mid-modiolar level (inferior part of the vestibule). The right saccule (small arrowhead) is slightly bigger than the utricle (marked with an arrowhead), but the vestibular structures are still separated. Compared with a left unaffected side, the saccule (marked with a thin arrow) is smaller than the utricle (marked with a thick arrow)

grade 1 CH in the Barath classification and a more robust enhancement of the cochlea were present.

In the sixth example (patient #6), a 45-year-old male with right-sided MD, the dilated confluent saccule and utricle pushed away the perilymphatic space, and no surrounding contrast structure was seen around them (Figure 8A). Using the Barath classification, it was classified as grade 2 VH and as grade 3 in the Bernaerts modification. The widening of endolymphatic vestibular structures was so signifi-

cant that they herniate into the posterior crus of the lateral semi-circular canal (Figure 8B). Moreover, CH grade 2 in the Barath classification with more robust PE was present.

In the seventh example (patient #7), a 68-year-old male with right-sided MD, on post-contrast 3D-FLAIR images no cochlear or vestibular EH was present, meaning grade 0 CH and grade 0 VH in both classifications, Barath and Bernaerts. Still, a robust PE of the cochlea was observed on the affected (right) side (Figure 9).

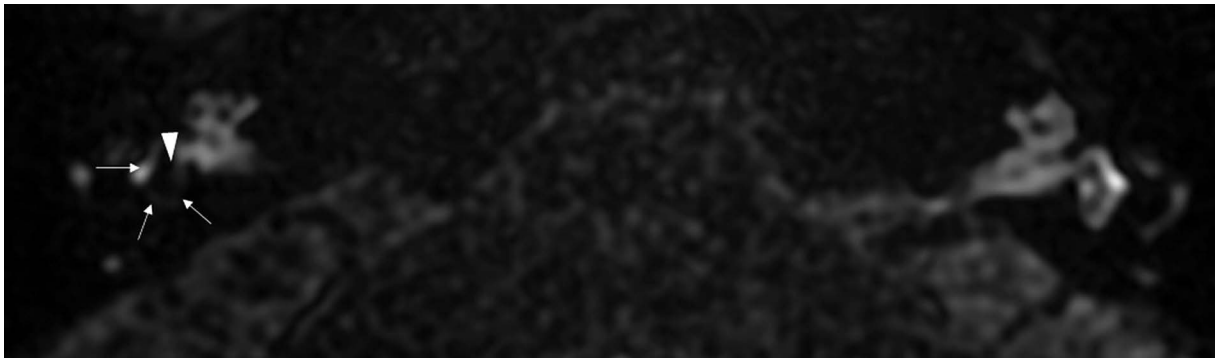


Figure 7. Magnetic resonance image of a 59-year-old female (patient #5) with right-sided clinically defined Ménière's disease. The example case of the mild vestibular hydrops – grade 2 in the Bernaerts scale [13] and grade 1 in the Barath grading system [11]. Delayed-postcontrast 3D-FLAIR T2 axial image of both ears below the mid-modiolar level (inferior part of the vestibule). On the right side, the saccule and utricle are enlarged and fused (arrowhead), but the enhancing rim of the vestibule's perilymphatic space is still visible (marked with arrows)

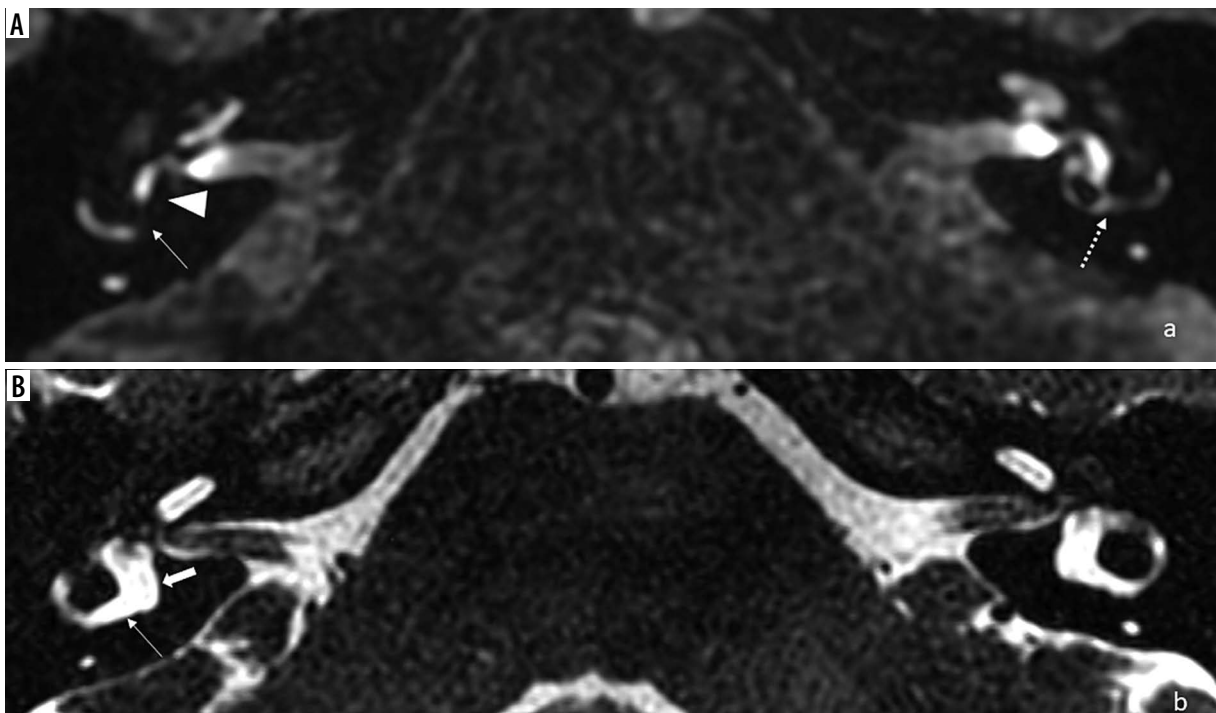


Figure 8. Magnetic resonance images of a 45-year-old male (patient #6) with right-sided clinically defined Ménière's disease. The example case of grade 2 vestibular hydrops according to the Barath classification [11] and grade 3 in the Bernaerts scale [13]. **A)** Delayed-postcontrast 3D-FLAIR T2 axial image of both ears below the mid-modiolar level (inferior part of the vestibule). No enhancing perilymphatic vestibular space is seen on the right. It is entirely encompassed by the widened, confluent endolymphatic saccule and utricle (marked with arrowhead). The endolymphatic hydrops herniation into the lateral semi-circular canal's posterior crus is visible (marked with an arrow). On the left side, the non-affected ear, the lateral semi-circular canal is preserved (marked with a dotted arrow). **B)** 3D-FIESTA axial image of both ears. Normal anatomy of the fluid-filled inner ear structures is visualized. The vestibule is marked with a thick arrow, posterior crus of the lateral semi-circular canal is marked with a thin arrow

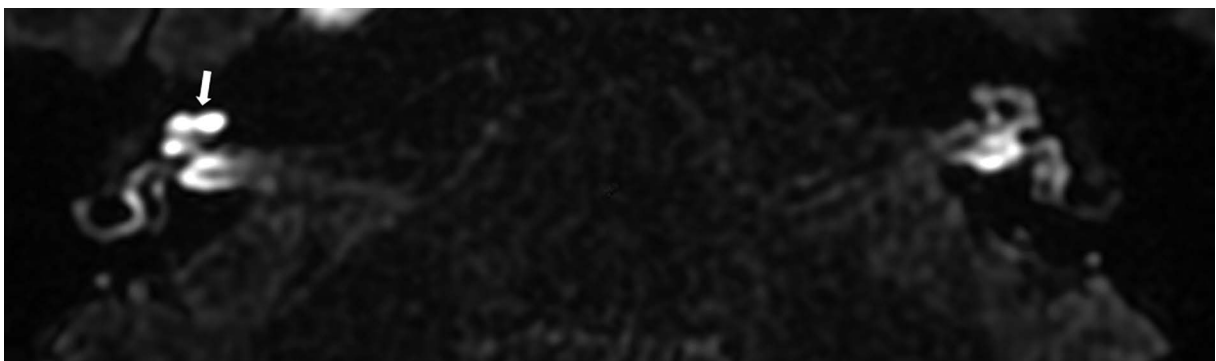


Figure 9. Magnetic resonance images of a 68-year-old male (patient #7) with right-sided clinically defined Ménière's disease. According to the Barath [11] and Bernaerts [13] classification, no signs of cochlear or vestibular endolymphatic hydrops are visible, classified as grade 0 in both scales. Delayed-postcontrast 3D-FLAIR T2 axial image of both ears at the mid-modiolar level revealed a more robust perilymphatic enhancement of cochlea on the affected (right) side (marked with an arrow)

Table 5. Magnetic resonance imaging findings in a group of patients with Ménière's disease. A cochlear hydrops was assessed using the Barath scale [11]. Vestibular hydrops was evaluated using the Barath [11] and Bernaerts [13] grading systems (VH grading in these 2 systems differ from each other, see Table 2). The degree of perilymphatic cochlear enhancement is presented

Case No.	Barath classification cochlea (grade 0, 1, or 2)	Barath classification vestibule (grade 0, 1, or 2)	Bernaerts classification vestibule (grade 0, 1, 2, or 3)	Degree of perilymphatic cochlear enhancement (equal/stronger)
1	0	0	0	Equal
2	1	1	2	Stronger
3	2	1	2	Stronger
4	0	0	1	Equal
5	1	1	2	Stronger
6	2	2	3	Stronger
7	0	0	0	Stronger

All the above-described imaging findings are summarized in Table 5.

Discussion

In our study, the usefulness of the well-known Barath scale [11] and a four-stage vestibular grading system recently described by Bernaerts [13] was illustrated in 7 example cases to present all possible MRI findings. It shows that MRI is a valuable and accurate EH visualization method that supports the MD's clinical diagnosis. The delayed post-contrast 3D-FLAIR sequence allows for the visualization of endolymphatic structures.

The first example patient with definite MD had no signs of any EH and no signs of increased PE of inner ear structures. Although EH is thought to be a hallmark of MD [3,4,11], controversies exist about whether the EH is a cause of MD or a result of an underlying pathology that leads to MD development [14-16]. Many post-mortem studies of temporal bones reported the presence of asymptomatic EH [15-19] as well as cases of MD without the EH [20-22]. These results are comparable with MRI studies. According to the literature [13,23,24], MRI does not reveal EH in 0-31% of patients with clinically diagnosed unilateral definite MD. Seo *et al.* [23] reported only one case without any EH within the group of 26 patients with MD (0.04%). In the Barath *et al.* [11] study, EH was not found in 5% (2/43) of affected ears, and in the Pakdaman *et al.* [24] study, EH was absent in 31% (10/32). These discrepancies might result from different EH assessment methods; some scientists used the semi-quantitative system proposed by Nakashima *et al.* [9], while others used the qualitative Barath system [11]. Furthermore, the MD duration in our first presented patient was not very long (6 years). The symptoms were mild; only weak vestibular symptoms were present, and the hearing was well preserved, which might explain the lack of visible changes within the inner ear. The impact of MD duration, the severity of symptoms, and the fluctuating character of MD in the presence of EH were analysed by Sepahdari *et al.* [25]

and Bernaerts *et al.* [13]. They reported the influence of MD duration on the grade of EH.

The next controversial issue is the pattern of EH development. In his meta-analysis of 184 temporal bone reports with EH, Pender [26] found that EH starts in the cochlear apex and then encompasses the saccule, utricle, ampullae, and canals. Other observations from MRI studies [11,27,28] questioned this theory because many studies found a higher prevalence of vestibular rather than CH in MD patients. Attye *et al.* [12] found that comparing vestibular structures to each other (saccule to utricle) increased the specificity of MD detection on MRI. Bernaerts *et al.* [13] confirmed that adding a saccule evaluation increases the sensitivity without loss of specificity for the diagnosis of definitive MD, and cochlear EH does not improve diagnostic accuracy. In addition, studies on the use of heavily T2-weighted images evaluate only VH [29,30]. Those MRI findings support saccular [12,31] rather than cochlea-centric theory for MD development.

A fourth example patient from our presented series is in line with the saccular theory. In this patient with normal hearing thresholds, no cochlear EH was present. However, the saccule was distended but was still separated from the utricle. On the Barath scales [11], this patient was classified as grade 0, which means no vestibular EH signs. By contrast, using the saccule-to-utricle ratio by Attye *et al.* [12] or four-stage VH by Bernaerts *et al.* [13], this case would be interpreted as abnormal, i.e. grade 1 VH on Bernaerts classification.

In our study, in the sixth example patient with severe VH, widened endolymphatic structures from the vestibulum herniated into the posterior, non-ampullated crus of the lateral semi-circular canal. A similar finding was described by Okuno and Sando [32] in MD patients' temporal bone specimens. Using MRI, the presence of this lesion was first reported by Gürkov *et al.* [33], who discovered that it correlates with an impaired caloric test. Recently, Sugimoto *et al.* [34] noticed that unilateral herniation is connected with EH progression.

Most of the patients in our group (5 of 7) had stronger PE of cochlea on the affected side. Two patients had equal PE on both sides; simultaneously, they did not have any CH signs. The first example patient had no signs of EH at all. The fourth example case had only VH. The increased inner-ear PE in MD was previously noted in various studies [11,24,35-37]. It is postulated that increased PE is related to increased blood-labyrinth barrier permeability [35,36]. Tagaya *et al.* [36] showed that the blood-labyrinth barrier is impaired in MD and that there is a correlation between EH and PE. In their study, all diseased ears presented stronger PE. Barath *et al.* [11] reported that the more robust contrast uptake was present in 90% of patients with EH. Conversely, Pakdaman *et al.* [24] compared blood-perilymph barrier permeability in MD patients with idiopathic sudden sensorineural hearing loss patients and found it to be higher in the MD group. They suggested that it might be a biomarker of MD. Recently, the value of cochlear PE in MD was proven by Bernaerts *et al.* [13]. They showed that PE assessment has high specificity and supports the diagnosis of MD. Furthermore, they proposed the diagnostic algorithm for unilateral MD. If the PE is more robust in the symptomatic ear, the ear can be classified as the MD ear, regardless of the presence of EH. The authors proved that this single factor has a higher inter-reader agreement than the clinical evaluation (0.79 vs. 0.66). In this context, our last patient (case example #7) is extremely interesting, with no EH signs but only with the cochlea's stronger PE on the symptomatic side. In this patient the dominating symptom was severe hearing loss, and the vestibular symptoms were not severe. In the literature, more robust PE enhancement was also described in patients with sudden deafness [38,39] and idiopathic sudden sensorineural hearing loss [24].

The main limitation of our study is the small number of patients; however, this is a pilot study, and we aimed to present the methodology and the most characteristic findings in a case series. Further studies with a larger group of patients are required. The second concern is the lack of a control group of healthy subjects. In our study, to evaluate endolymphatic hydrops, we chose the qualitative scale where each ear is assessed separately; therefore,

there was no need to compare them to healthy controls. According to the Bernaerts criteria [13], each patient's affected ears and the contralateral ears were evaluated when assessing the perilymphatic enhancement of the cochlea as it is included in the criteria. Still, it does not mean that the contralateral ears were considered entirely healthy. The contralateral ears in our patients were asymptomatic and presented normal test results. However, it should be kept in mind that endolymphatic hydrops can develop for years in the contralateral ear in patients with unilateral MD before clinical symptoms from that ear start [24,40]. Moreover, using a double dose of contrast media in healthy volunteers might be ethically controversial, and there was no Ethics Committee approval for that.

Conclusions

In patients with MD, endolymphatic hydrops can be studied on MRI using 3D-FLAIR delayed post-contrast images. The qualitative Barath [11] grading system may be easily used in EH assessment. Bernaerts *et al.* [13] recently described new radiological signs of MD, such as increased perilymphatic enhancement of the cochlea, and an extra low-grade VH would be worth adding to the MRI assessment of EH. It might increase the diagnosis sensitivity of MD. MRI supports not only the clinical diagnosis of MD but also helps to understand its pathophysiology.

Statement of ethics

The local Ethics Committee reviewed and approved the study protocol at the institution where the study was conducted (KB/110/2019). The project conforms to the Code of Ethics of the World Medical Association (Declaration of Helsinki). All patients gave their written informed consent for participation in the study.

Conflict of interest

The authors report no conflict of interest.

References

1. Goebel JA. 2015 Equilibrium Committee amendment to the 1995 AAO-HNS guidelines for the definition of Meniere's disease. *Otolaryngol Head Neck Surg* 2016; 154: 403-404.
2. Meniere P. Maladies de l'oreille interne offrant les symptômes de la congestion cérébrale apoplectiforme. *Gaz Med Paris* 1861; 16: 88-89.
3. Hallpike CS, Cairns H. Observations on the pathology of Ménière's syndrome. *Proc R Soc Med* 1938; 31: 1317-1336.
4. Yamakawa K. Über die pathologische Veränderung bei einem Ménière-Kranken. *J Otorhinolaryngol Soc Jpn* 1938; 4: 2310-2312.
5. Committee on Hearing and Equilibrium guidelines for the diagnosis and evaluation of therapy in Meniere's disease. American Academy of Otolaryngology-Head and Neck Foundation, Inc. *Otolaryngol Head Neck Surg* 1995; 113: 181-185.
6. Lopez-Escamez JA, Carey J, Chung WH, et al. Diagnostic criteria for Meniere's disease. *J Vestib Res* 2015; 25: 1-7.
7. Nakashima T, Naganawa S, Sugiura M, et al. Visualization of endolymphatic hydrops in patients with Meniere's disease. *Laryngoscope* 2007; 117: 415-420.

8. Nakashima T, Naganawa S, Teranishi M, et al. Endolymphatic hydrops revealed by intravenous gadolinium injection in patients with Ménière's disease. *Acta Otolaryngol* 2010; 130: 338-343.
9. Nakashima T, Naganawa S, Pyykko I, et al. Grading of endolymphatic hydrops using magnetic resonance imaging. *Acta Otolaryngol Suppl* 2009; (560): 5-8.
10. Gurkov R, Berman A, Dietrich O, et al. MR volumetric assessment of endolymphatic hydrops. *Eur Radiol* 2015; 25: 585-595.
11. Barath K, Schuknecht B, Naldi AM, et al. Detection and grading of endolymphatic hydrops in Meniere disease using MR imaging. *AJNR Am J Neuroradiol* 2014; 35: 1387-1392.
12. Attye A, Eliezer M, Boudiaf N, et al. MRI of endolymphatic hydrops in patients with Meniere's disease: a case-controlled study with a simplified classification based on saccular morphology. *Eur Radiol* 2017; 27: 3138-3146.
13. Bernaerts A, Vanspauwen R, Blavie C, et al. The value of four stage vestibular hydrops grading and asymmetric perilymphatic enhancement in the diagnosis of Meniere's disease on MRI. *Neuroradiology* 2019; 61: 421-429.
14. Rauch SD, Merchant SN, Thedinger BA. Meniere's syndrome and endolymphatic hydrops. Double-blind temporal bone study. *Ann Otol Rhinol Laryngol* 1989; 98: 873-883.
15. Merchant SN, Adams JC, Nadol JB Jr. Pathophysiology of Meniere's syndrome: are symptoms caused by endolymphatic hydrops? *Otol Neurotol* 2005; 26: 74-81.
16. Foster CA, Breeze RE. Endolymphatic hydrops in Ménière's disease: cause, consequence, or epiphenomenon? *Otol Neurotol* 2013; 34: 1210-1214.
17. Schuknecht HF, Gulya AJ. Endolymphatic hydrops. An overview and classification. *Ann Otol Rhinol Laryngol Suppl* 1983; 106: 1-20.
18. Vasama JP, Linthicum FH Jr. Meniere's disease and endolymphatic hydrops without Meniere's symptoms: temporal bone histopathology. *Acta Otolaryngol* 1999; 119: 297-301.
19. Belal A Jr, Antunez JC. Pathology of endolymphatic hydrops. *J Laryngol Otol* 1980; 94: 1231-1240.
20. Arnvig J. Histological findings in a case of Ménière's disease with remarks on the pathologic-anatomic basis of this lesion. *Acta Otolaryngol* 1947; 35: 453-466.
21. Belal A, Ylikoski J. Pathologic significance of Ménière's symptom complex: a histopathologic and electron microscopic study. *Am J Otolaryngol* 1980; 1: 275-284.
22. Frayssé BG, Alonso A, House WF. Meniere's disease and endolymphatic hydrops: clinical-histopathological correlations. *Ann Otol Rhinol Laryngol Suppl* 1980; 89 (6 Pt 3): 2-22.
23. Seo YJ, Kim J, Choi JY, Lee WS. Visualization of endolymphatic hydrops and correlation with audio-vestibular functional testing in patients with definite Meniere's disease. *Auris Nasus Larynx* 2013; 40: 167-172.
24. Pakdaman MN, Ishiyama G, Ishiyama A, et al. Blood-labyrinth barrier permeability in Meniere disease and idiopathic sudden sensorineural hearing loss: findings on delayed postcontrast 3D-FLAIR MRI. *AJNR Am J Neuroradiol* 2016; 37: 1903-1908.
25. Sepahdari AR, Ishiyama G, Vorasubin N, et al. Delayed intravenous contrast-enhanced 3D FLAIR MRI in Meniere's disease: correlation of quantitative measures of endolymphatic hydrops with hearing. *Clin Imaging* 2015; 39: 26-31.
26. Pender DJ. Endolymphatic hydrops and Ménière's disease: a lesion meta-analysis. *J Laryngol Otol* 2014; 128: 859-865.
27. Pyykko I, Nakashima T, Yoshida T, et al. Meniere's disease: a reappraisal supported by a variable latency of symptoms and the MRI visualisation of endolymphatic hydrops. *BMJ Open* 2013; 3: e001555.
28. Attye A, Dumas G, Tropres I, et al. Recurrent peripheral vestibulopathy: is MRI useful for the diagnosis of endolymphatic hydrops in clinical practice? *Eur Radiol* 2015; 25: 3043-3049.
29. Venkatasamy A, Veillon F, Fleury A, et al. Imaging of the saccule for the diagnosis of endolymphatic hydrops in Meniere disease, using a three-dimensional T2-weighted steady state free precession sequence: accurate, fast, and without contrast material intravenous injection. *Eur Radiol Exp* 2017; 1: 14.
30. Simon F, Guichard JP, Kania R, et al. Saccular measurements in routine MRI can predict hydrops in Ménière's disease. *Eur Arch Otorhinolaryngol* 2017; 274: 4113-4120.
31. Morita N, Kariya S, Farajzadeh Deroee A, et al. Membranous labyrinth volumes in normal ears and Ménière disease: a three-dimensional reconstruction study. *Laryngoscope* 2009; 119: 2216-2220.
32. Okuno T, Sando I. Localization, frequency, and severity of endolymphatic hydrops and the pathology of the labyrinthine membrane in Ménière's disease. *Ann Otol Rhinol Laryngol* 1987; 96: 438-445.
33. Gurkov R, Flatz W, Louza J, et al. Herniation of the membranous labyrinth into the horizontal semicircular canal is correlated with impaired caloric response in Ménière's disease. *Otol Neurotol* 2012; 33: 1375-1379.
34. Sugimoto S, Yoshida T, Teranishi M, et al. Significance of endolymphatic hydrops herniation into the semicircular canals detected on MRI. *Otol Neurotol* 2018; 39: 1229-1234.
35. Zou J, Poe D, Bjelke B, Pyykko I. Visualization of inner ear disorders with MRI in vivo: from animal models to human application. *Acta Otolaryngol Suppl* 2009 (560): 22-31.
36. Tagaya M, Yamazaki M, Teranishi M, et al. Endolymphatic hydrops and blood-labyrinth barrier in Ménière's disease. *Acta Otolaryngol* 2011; 131: 474-479.
37. Yamazaki M, Naganawa S, Tagaya M, et al. Comparison of contrast effect on the cochlear perilymph after intratympanic and intravenous gadolinium injection. *AJNR Am J Neuroradiol* 2012; 33: 773-778.
38. Tagaya M, Teranishi M, Naganawa S, et al. 3 Tesla magnetic resonance imaging obtained 4 hours after intravenous gadolinium injection in patients with sudden deafness. *Acta Otolaryngol* 2010; 130: 665-669.
39. Lee HY, Jung SY, Park MS, et al. Feasibility of three-dimensional fluid-attenuated inversion recovery magnetic resonance imaging as a prognostic factor in patients with sudden hearing loss. *Eur Arch Otorhinolaryngol* 2012; 269: 1885-1891.
40. Balkany TJ, Sires B, Arenberg IK. Bilateral aspects of Meniere's disease: an underestimated clinical entity. *Otolaryngol Clin North Am* 1980; 13: 603-609.